Patchy nanoparticles with surface complexity for directed self-assembly

Thi Vo*

Patchy nanoparticles (PNPs) possess anisotropic surfaces that produce emergent directionalities in interactions. Manipulation of such surface complexities offers a powerful handle for control over interparticle spatial and orientational orderings, making PNPs an ideal class of nanoscale synthons for self-assembly. However, realization of PNPs with defined patch positions and geometries faces technical challenges related to the level of precision chemistry required to achieve the desired surface patterning. Here, we provide an in-depth review of state-of-the-art strategies available for PNP synthesis. We examine the experimental efforts made to synthesize PNPs, classifying advances based on different material types spanning organic and inorganic systems. We conclude by presenting barriers in PNP synthesis and highlighting ongoing theoretical efforts aimed at guiding experimental design and parameter selection for creating novel surface patterning on NPs.
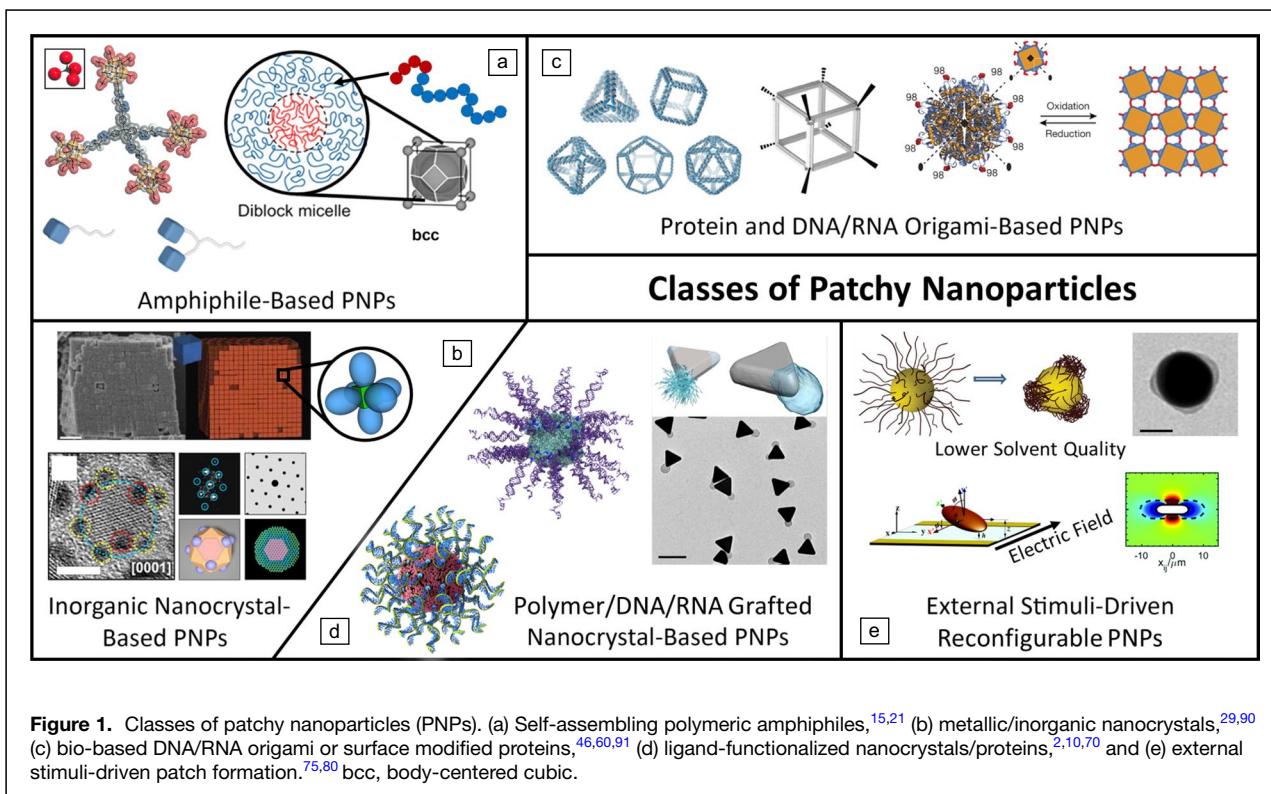
Introduction

Leveraging self-assembly to *a priori* direct building-block organization provides a powerful design paradigm for creating spatially and orientationally ordered superlattices.[1–3] Nanoparticles (NPs) are of particular interest as they exhibit a diverse range of optical,[4] magnetic,[5] and/or catalytic[6] properties. Attempts to direct NP self-assembly have produced a diverse suite of strategies that include templating via solvent crystallization,[7,8] surface modifications,[9,10] and microphase separation.[11] Among these approaches, surface modifications have emerged as an effective strategy capable of producing ordered co-assemblies of incompatible NPs.[1–3] However, to date, self-assembled lattices accessible via this approach are limited to "close-packed" morphologies. This constraint stems from the isotropic nature of inter-NP, which favors morphologies with high symmetry and high packing fraction.

The promise of patchy particles for directed self-assembly

Efforts to bypass the "close-packed" limitations have sparked interest in designing NPs capable of breaking high coordination symmetry. Low-density (coordination) lattices have been predicted to exhibit photonic bandgaps, useful for optical waveguides, optical computing, sensors, and telecommunications.[12] Similarly, simulations have shown that porous materials with tunable pore sizes can exhibit encapsulation and filtration capabilities, ideal for membrane applications.[13] Finally, designs of porous lattices made from metal–organic frameworks have highlighted structural motifs that exhibit superior catalytic properties.[14] The common thread across these works lies in directional interactions that break isotropic symmetry, thereby favoring more open configurations. Such patchy NPs (PNPs) are anisotropic by nature, either via selective surface modification or via alteration of their geometry. Successful design and synthesis of PNPs can provide a powerful bottom-up approach to experimentally realize materials capable of satisfying current technological demands. Attempts to synthesize PNPs have produced a suite of experimental works spanning organic and inorganic systems and even leverage external stimuli to control patch formation. Due to the expansive nature of the experimental literature, we organize PNPs into categories: (1) soft PNPs from oligomeric and/or polymeric amphiphiles, (2) PNPs made from inorganic nanocrystals, (3) bio-based PNPs obtained from proteins or DNA/RNA origami, (4) PNPs created from ligand functionalization onto proteins/NPs, and (5) reconfigurable PNPs via solvent/external field manipulations (**Figure 1**).

Figure 1. Classes of patchy nanoparticles (PNPs). (a) Self-assembling polymeric amphiphiles,[15,21] (b) metallic/inorganic nanocrystals,[29,90] (c) bio-based DNA/RNA origami or surface modified proteins,[46,60,91] (d) ligand-functionalized nanocrystals/proteins,[2,10,70] and (e) external stimuli-driven patch formation.[75,80] bcc, body-centered cubic.
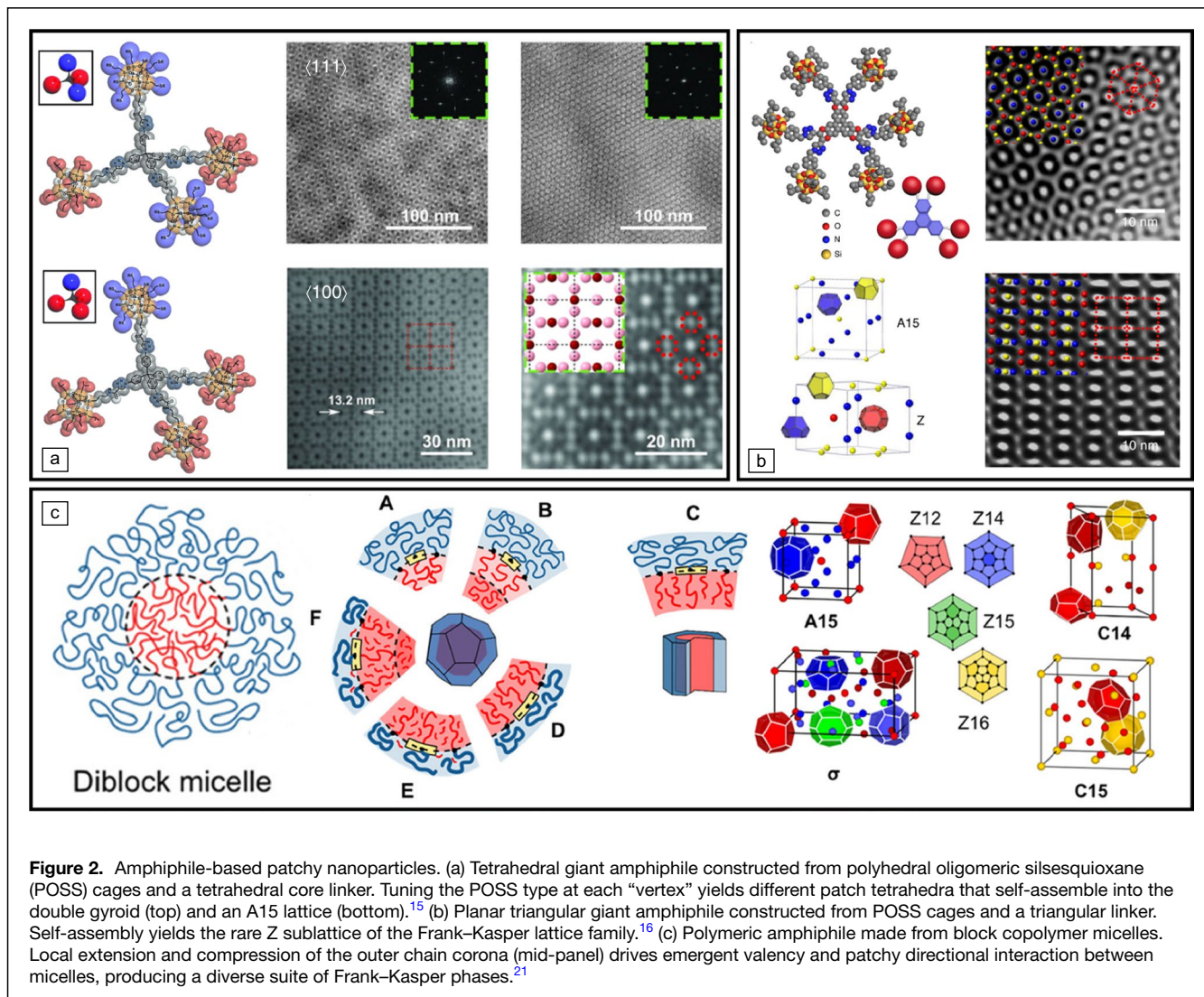
PNPs from oligomeric and polymeric amphiphiles

Amphiphiles represent a class of materials containing incompatible subunits that, if tuned correctly, can direct self-assembly into ordered superlattices/motifs. Interactions between individual amphiphiles can be engineered via leveraging the molecular geometry of their subunits to create steric hindrance or chemical specific attraction/repulsion that biases alignment along a specific direction. Amphiphiles constructed using this design strategy are classified as giant amphiphiles due to the bulky nature of the individual subunits. Combining a rigid tetrahedral molecule functionalized with polyhedral oligomeric silsesquioxane (POSS) (and POSS-derivatives) at each vertices imbues the resulting amphiphile with an emergent fourfold interaction[15] (**Figure 2**a). Because the core and the POSS particles favor segregation, the net result is a soft tetrahedral PNP with vertex–vertex attraction. The POSS particles at each vertex of the tetrahedral core can also be altered to control specific vertex–vertex interactions, providing a tunable tetrahedral PNP made from molecular amphiphiles. For this specific system, tetrahedral PNPs self-assemble into the A15, dodecagonal quasicrystalline, lamellar, double gyroid, and hexagonal cylindrical lattices by tuning the functionalized POSS hydrophobic/hydrophilic interactions. Another example is vertex patchy triangular PNPs synthesized using a triphenylene core and BPOSS vertices, which assemble into Laves structures[16] (Figure 2b). Utilizing POSS particle as the core produces

vertex patchy cubic PNPs that self-assemble into a suite of different structures ranging from simple cubic lattices to quasicrystalline structures, again depending on the specific vertex–vertex interaction.[17] Cores made from aromatic rings create giant molecules where π-π stacking dominate, producing para-like patchy PNPs capable of forming Frank–Kasper phases.[18] These examples indicate that engineering of giant molecules can provide a powerful handle to fabricate molecularly precise PNPs of varying shapes and sizes.[19]

Traditional polymeric amphiphiles themselves can be engineered to self-assemble into interesting soft PNPs; for example, diblock copolymers typically form spherical micellar motifs in the limit of high asymmetry in lengths between the two sub-blocks. Seminal works in self-assembly of hard and soft systems have shown that spherical particles assemble into a body-centered-cubic (bcc) or face-centered-cubic (fcc) lattice.[20] However, introduction of free core-homopolymer into the system shifts assembly behavior to drive the formation of more complex Frank–Kasper, σ, C14, C15, and dodecagonal quasicrystalline lattices[21] (Figure 2c). This is because the free core-homopolymer drives reorganization of the spherical micelles, altering their effective shape into anisotropic variants exhibiting directional interactions. Such emergent PNPs from a starting spherical micellar motif have also been observed in ionic-driven systems.[22] Furthermore, analogous strategies have been used to convert spherically symmetric micelles to exhibit para-patchy interactions that then shift assembly into strings and network structure.[23]

Figure 2. Amphiphile-based patchy nanoparticles. (a) Tetrahedral giant amphiphile constructed from polyhedral oligomeric silsesquioxane (POSS) cages and a tetrahedral core linker. Tuning the POSS type at each "vertex" yields different patch tetrahedra that self-assemble into the double gyroid (top) and an A15 lattice (bottom).[15] (b) Planar triangular giant amphiphile constructed from POSS cages and a triangular linker. Self-assembly yields the rare Z sublattice of the Frank–Kasper lattice family.[16] (c) Polymeric amphiphile made from block copolymer micelles. Local extension and compression of the outer chain corona (mid-panel) drives emergent valency and patchy directional interaction between micelles, producing a diverse suite of Frank–Kasper phases.[21]

PNPs from inorganic nanocrystals

Inorganic PNPs use anisotropic metal NPs such as Au, Ag, Pt, and/or Pd. Over the past decade, major advances in synthesis and growth of nanocrystals have led to the proliferation of a diverse suite of shaped NPs. There are many excellent reviews on chemical synthesis of anisotropic NPs and we refer the reader to those works for details.[1,24] Here, we focus on features of anisotropic NPs that contribute to their applicability for PNPs.

First, anisotropic NPs have surfaces of varying curvatures. This means that differences in local curvature between one location versus another can result in emergent directional interactions. Seminal works in theory and simulations have shown that anisotropic shapes exhibit preferred orientational alignments at moderate to high particle volume fraction that arises due to entropy.[25–27] For example, a cubic NP will exhibit strong preferences for face-face alignment. The net effect is a face patchy cubic PNP that arises purely from geometry. Experiments taking advantage of this emergent "patchiness"

have successfully self-assembled a wide range of crystalline lattices, including a simple cubic lattice from cubic NPs,[28] a Minkowski lattice from octahedral NPs,[29] a bcc from cuboctahedral NPs,[30] and chiral or quasicrystalline lattices using tetrahedral NPs.[31,32] The same emergent patchy valency is also observed in assemblies under two-dimensional (2D) confinement of nanoplates, where here the edge serves as the largest "facet" on the NPs.[33,34]

The key limitation for hard shapes, however, lies in the bias toward close-packed structures. This is because entropically driven processes minimize excluded volume between particles, which is analogous to seeking configurations that occupy the smallest space within the self-assembled structures.[35] One synthetic strategy seeking to bypass this constraint for metal NPs is the construction of heterostructural NPs: that is, NPs surface decorated with smaller NP satellite(s). Such NPs are typically synthesized via sequential seeded growth, where preformed NPs serve as seed sites to grow larger NPs.[36] This process results in composite NPs such as heterodimers,

heterotrimers, etc. These heterostructural NPs are patchy by construction as the small NP satellites imbue local directional interactions. This process forgoes the need to rely on emergent patchiness between anisotropic NPs due to geometry in favor of explicit surface patchiness defined by NP satellites. Although heterostructural NP self-assembly is less explored compared to standard NP superlattices, interesting structures have already been observed. Examples include the tunability between rotator, aligned, and disordered fcc phases for a Pt-Fe_3O_4 heterodimer[37] (**Figure 3**a), fcc packing of a quantum dot (QD)-Au heterodimer exhibiting a unique orientational ordering[38] (Figure 3c), and fcc packings of 4-/5-/6-patched QD-Au heterostructural NPs that exhibit tunable voids shape (Figure 3b).[39]

Bio-based PNPs

Inorganic synthesis is constrained by polydispersity,[1,40] where variations in the size/shape of the NP cores can disrupt preprogrammed PNP interactions and create defects/disorder in the assembled superlattices.[1,3,41,42] Proteins, on the other hand, are monodispersed. More importantly, protocols exist that enable precision modification of amino acid residues on the protein's surface to reprogram protein–protein interactions.[43] This means that a positively charged surface site can be switched to be negatively charged, neutral, hydrophobic, or hydrophilic depending on the replacement amino acid. The net result is tunable directional interactions via protein surface modification. Designing protein-based PNPs has led to a large suite of interesting self-assembled morphologies that emulate the natural diversity in protein shape/size/ interaction seen in nature. For example, surface modification of L-rhamnulose-1-phosphate aldolase breaks the packing symmetry of the core protein, producing porous structures[44] (**Figure 4**d). Designing patchy protein helical bundles has also been achieved where the proteins behave analogous to divalent, para-patchy cylinders, directing self-assembly into micron-length rods with varying degrees of flexibility.[45] Porous, 2D protein arrays have also been achieved by designing directional interactions that maximize protein–protein interfacial binding required to stabilize various structures[46,47] (Figure 4a). This ability to define, select, and synthesize the exact patch locations on a particle surface is a holy grail for PNP design. Numerous examples of other designer patchy proteins exist that are capable of self-assembling into one-dimensional strings/fibers,[48,49] 2D sheets/arrays,[50,51] and three-dimensional protein cages.[52,53]

In recent years, DNA/RNA origami has risen to the top as a powerful strategy for designing tailorable PNPs. Origami takes advantage of complementary base pairing between DNAs and RNAs to direct chain organization into hierarchical structures.[54,55] In applying origami principles for PNPs, one approach defines a unique single-stranded DNA sequence that protrudes out of a self-assembled DNA origami structure.[3] For example, DNA origami tetrahedral nanocages can be desi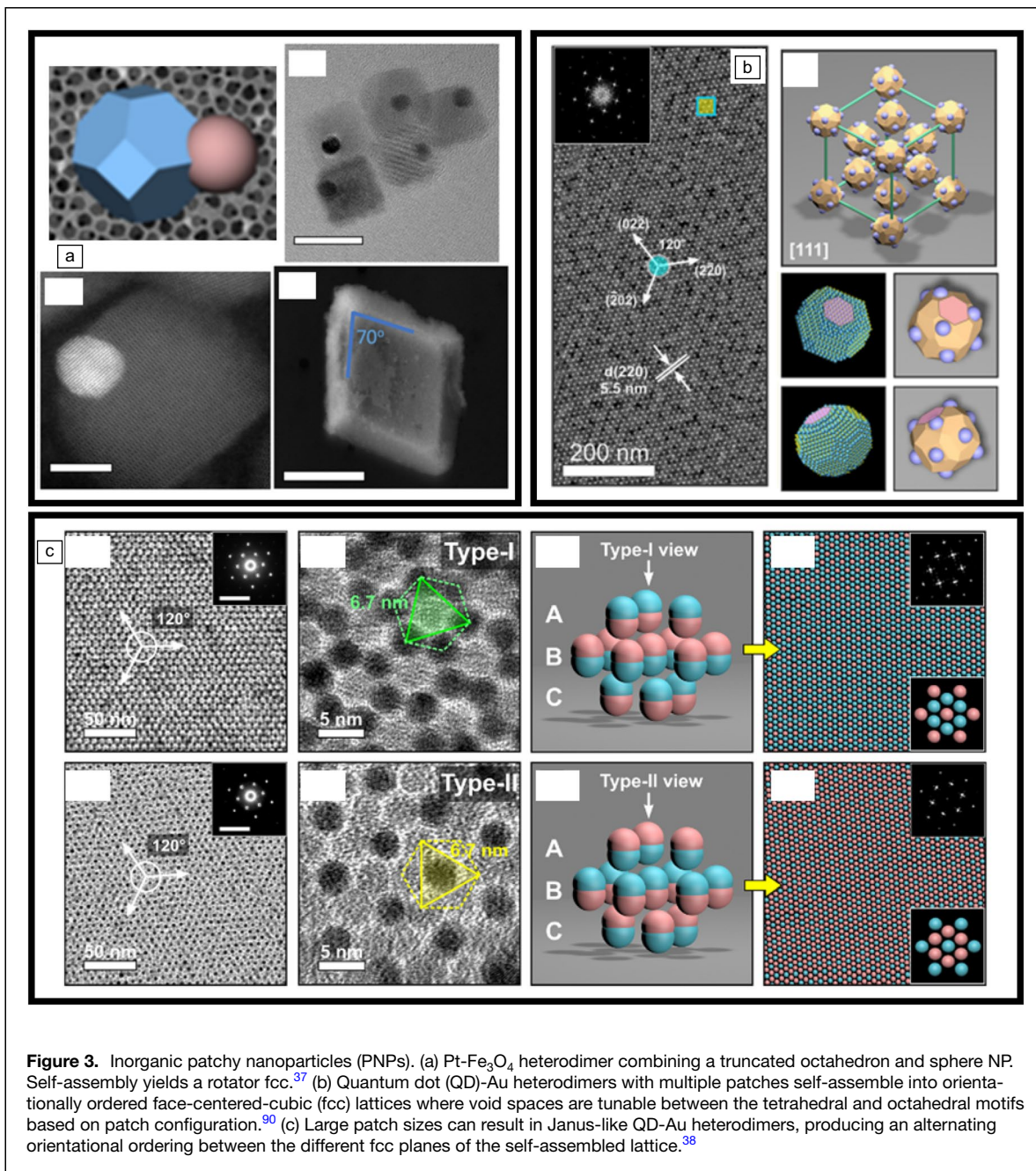gned to have complementary sticky ends at their vertices. This will result in tetrahedral particles whose vertices are attractive to each other via DNA hybridization: equivalent to a vertex patched tetrahedral PNP. The same strategy can also utilize RNA hybridization[56] (Figure 4c). To date, there are numerous examples where DNA/RNA origami has been utilized to create PNPs for directed self-assembly.[3,57] Of particular interest are DNA origami cages that self-assemble into low coordination or porous structures such as strings/fibers,[58] open bcc or SC superlattices[59,60] (Figure 4b), porous fcc superlattices,[61] and nanoscale diamond superlattice.[62] All examples utilize vertex patched octahedral, cubic, or tetrahedral nanocages as the PNP building blocks. While the self-assembled structures are different, PNP synthesis process remains the same, making DNA origami a versatile tool with precision control over patch arrangement on NPs.

PNPs from ligand functionalization

Ligand-functionalized NPs (LNPs) incorporate a wide range of different ligand species that include molecules,[63] oligomers/polymers,[64] or DNA/RNA.[1–3,65] The NPs can encompass inorganic materials such as metallic nanocrystals or biological materials such as proteins. Covering the entire suite of LNPs is beyond the scope of this article and we refer the reader to multiple excellent reviews on these materials.[1,3,65] Our scope focuses on LNPs that exhibit patchy/complex ligand surface patterning to elicit directional interactions.

Ligand functionalization often faces limitation in precision control over where ligands are anchored on the NP surfaces. This is because all NP surface locations are chemically equivalent. The usage of anisotropic NPs offers more precision in ligand functionalization as chain entropy drives local partitioning toward locations of high surface curvatures.[66,67] However, such partitioning is restricted to geometrically equivalent sites. One strategy that bypasses these limitations utilizes protection groups to "block" functionalization at different surface sites.[68] Free ligands are first introduced that physisorb to the particle surface. Once "protected," ligand functionalization can progress on the "unprotected" surface sites and the physisorbed chain can be washed off post-functionalization. The net result is a LNP with ligand functionalization on only certain surface sites, making it a PNP (**Figure 5**a). However, the initial coating is still controlled by random, chain adsorption, making precision control over the final patch location an open challenge.

A corollary approach to the previously discussed surface blocking strategy is to utilize DNA nanocages to lock NP orientation before functionalization.[69] In this limit, the NP is first captured and held in place by a DNA nanocage. Depending on the nanocage geometry, different locations of the cargo NP are exposed to DNA/ligand functionalization. For example, a cubic nanocage will produce a six-patch PNP, where each patch sits at the face location of the cubic nanocage. Conversely, a tetrahedral nanocage will only yield a four-patch PNP (Figure 5b). This process provides more control over
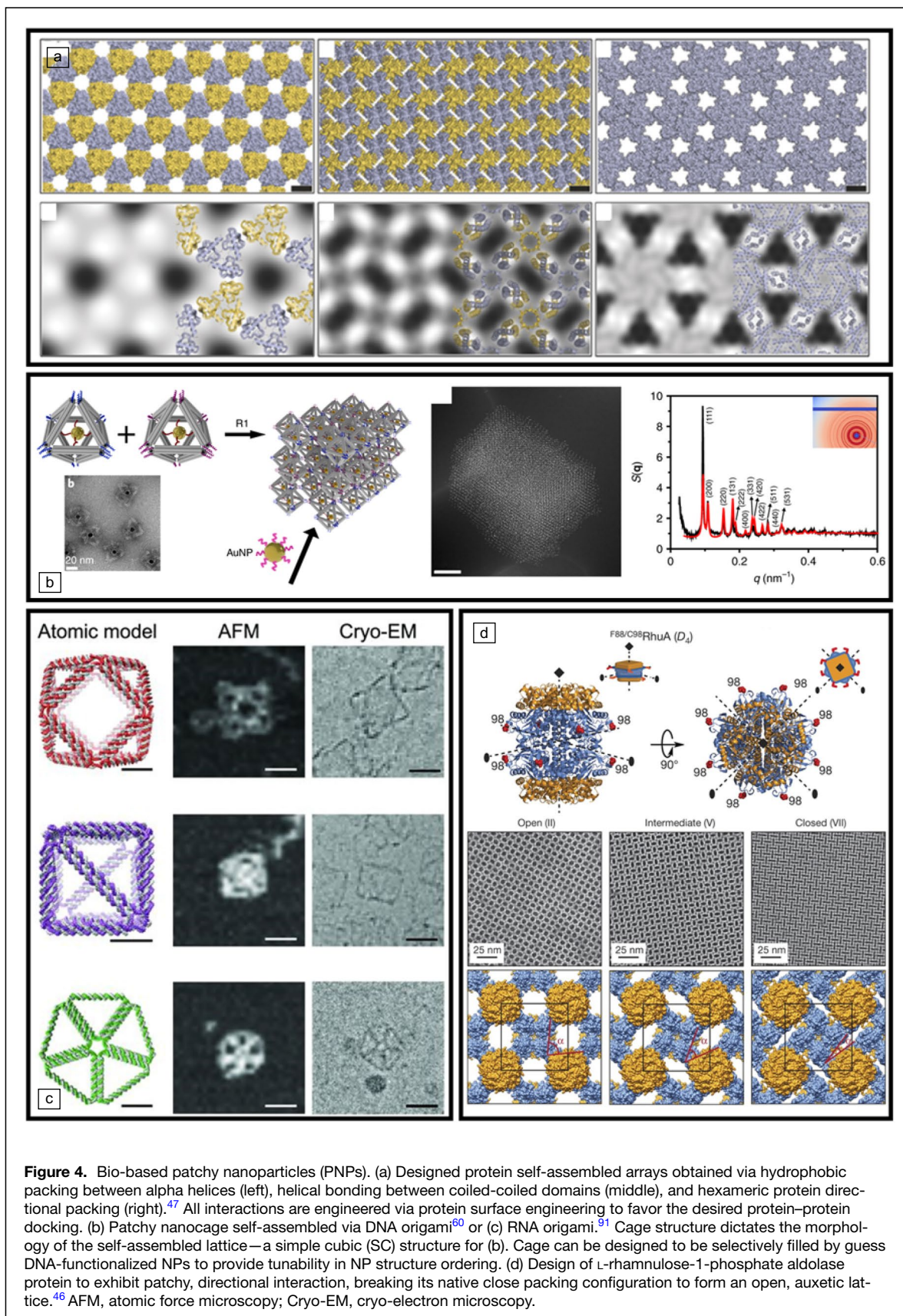
Figure 3. Inorganic patchy nanoparticles (PNPs). (a) Pt-Fe$_3$O$_4$ heterodimer combining a truncated octahedron and sphere NP. Self-assembly yields a rotator fcc.[37] (b) Quantum dot (QD)-Au heterodimers with multiple patches self-assemble into orientationally ordered face-centered-cubic (fcc) lattices where void spaces are tunable between the tetrahedral and octahedral motifs based on patch configuration.[90] (c) Large patch sizes can result in Janus-like QD-Au heterodimers, producing an alternating orientational ordering between the different fcc planes of the self-assembled lattice.[38]

where patches are created, but self-assembly of such patterned PNPs has not yet been tested.

Rather than "protecting" the NP surface, another strategy utilizes protein surface heterogeneity to selectively control surface functionalization.[70] This heterogeneity enables ligand functionalization at a precisely defined position on the protein's surface to produce complex protein-based PNPs. Due to the precision of such a protocol, the synthesized functionalized proteins have been shown to self-assemble into a diverse range of superlattices. Experiments have shown that switching the DNA functionalization site on concanavalin A alters their orientation alignment and
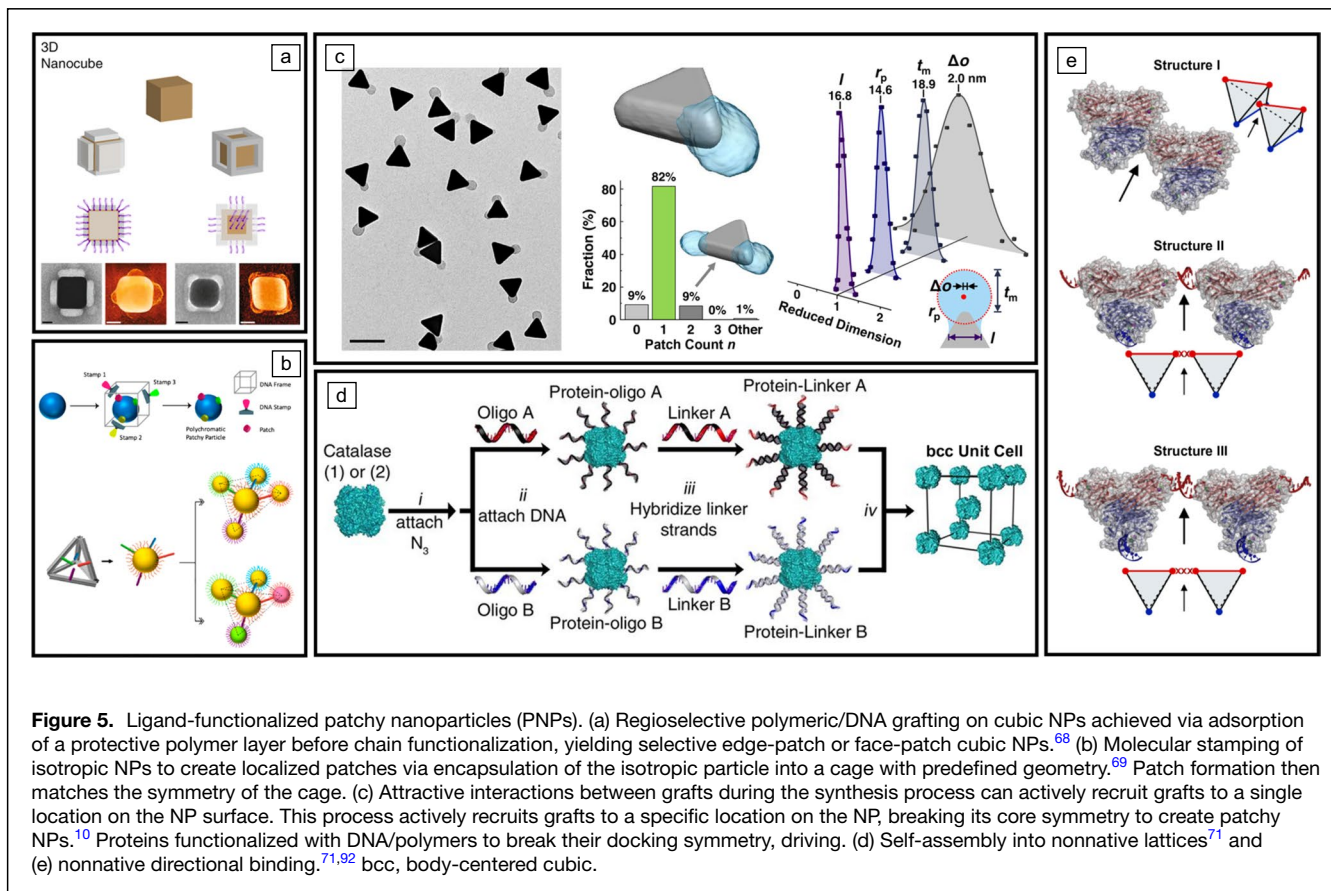
enables a systematic transition across five self-assembled structures[71] (Figure 5e). Similarly, switching DNA functionalization locations on a hexameric protein shifts assemblies between rods and sheets formation.[72] Superlattices such as SC, bcc, and layered hexagonal morphologies have also been reported by tuning DNA functionalization on the protein surfaces[73] (Figure 5d).

Finally, ligand–ligand interactions can serve as a powerful handle to synthesize PNPs. Increasing chain–chain attraction between functionalized ligands can produce partitioning to specific sites on NP surfaces.[10] Specifically, the first physisorbed ligand on an NP actively recruits nearby ligands to the

Figure 4. Bio-based patchy nanoparticles (PNPs). (a) Designed protein self-assembled arrays obtained via hydrophobic packing between alpha helices (left), helical bonding between coiled-coiled domains (middle), and hexameric protein directional packing (right).[47] All interactions are engineered via protein surface engineering to favor the desired protein–protein docking. (b) Patchy nanocage self-assembled via DNA origami[60] or (c) RNA origami.[91] Cage structure dictates the morphology of the self-assembled lattice—a simple cubic (SC) structure for (b). Cage can be designed to be selectively filled by guess DNA-functionalized NPs to provide tunability in NP structure ordering. (d) Design of L-rhamnulose-1-phosphate aldolase protein to exhibit patchy, directional interaction, breaking its native close packing configuration to form an open, auxetic lattice.[46] AFM, atomic force microscopy; Cryo-EM, cryo-electron microscopy.

Figure 5. Ligand-functionalized patchy nanoparticles (PNPs). (a) Regioselective polymeric/DNA grafting on cubic NPs achieved via adsorption of a protective polymer layer before chain functionalization, yielding selective edge-patch or face-patch cubic NPs.[68] (b) Molecular stamping of isotropic NPs to create localized patches via encapsulation of the isotropic particle into a cage with predefined geometry.[69] Patch formation then matches the symmetry of the cage. (c) Attractive interactions between grafts during the synthesis process can actively recruit grafts to a single location on the NP surface. This process actively recruits grafts to a specific location on the NP, breaking its core symmetry to create patchy NPs.[10] Proteins functionalized with DNA/polymers to break their docking symmetry, driving. (d) Self-assembly into nonnative lattices[71] and (e) nonnative directional binding.[71,92] bcc, body-centered cubic.

same surface region, creating an emergent symmetry breaking in functionalization. Applications of this strategy have resulted in the formation of singlet, doublet, and triplet patches on triangular prism NPs[10] (Figure 5c) as well as an octahedrally configured set of six patches on spherical NPs.[74] Both examples indicate that introducing chain–chain interactions can serve as an effective synthetic strategy to break geometric constraints imposed by the NP core to enable tunability in surface patterning.

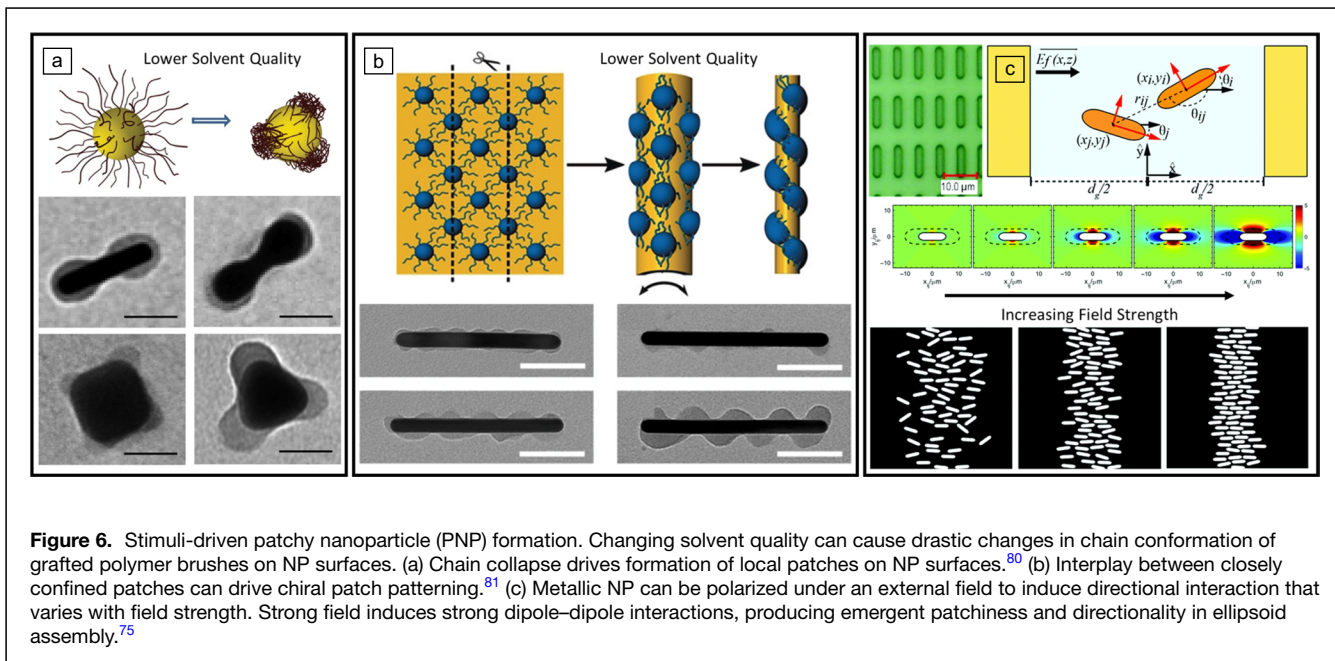### Reconfigurable PNPs via external stimuli

Since inorganic NPs are mostly made from metallic atomic nanocrystals, external fields (i.e., electric or magnetic) can polarize the NP and induce dipole–dipole interactions between neighboring particles. At low field strength, this induced dipole interaction is weak. However, at high enough field strengths, this term will dominate to produce emergent directional interactions.[75,76] For these reasons, we classify these cases as inducible valency/patchiness. Experimental measurements have shown that isotropic, spherical NPs will exhibit para-like patches due to dipole–dipole interactions. Similarly, ellipsoidal/anisotropic NPs will develop para-like patches along their long axis[75,77,78] (**Figure 6**c). The net effect is the emergence of a field-induced PNP formation that directly alters particle assembly behaviors.

Solvent-induced patch formation leverages the switching of good to poor solvent to shape the covalently end-functionalized ligand distribution about the NP core. Due to the change in solvent quality, the functionalized polymers will shift from a solvated, wetted state to a collapsed state to minimize unfavorable chain–solvent interaction. However, due to its covalently linked tail to the NP surface, full segregation is not possible. As such, the next best possible option is to hug the NP surface and stretch as much as it can to contact with a surface region containing higher polymer concentration. While this requires a large cost in entropy, the enthalpic gain from chain–chain interaction makes this process favorable and produces localized patchy polymer brushes on the NP. Application of this strategy has produced edge/corner patchy cubic NPs[79] (Figure 6a), patchy octahedral NPs, patches on spherical NPs,[80] and chiral patches on rod-like NPs[81] (Figure 6b).

Outlook and limitations

With respect to ligand-functionalized NPs, more robust methods are needed to increase selectivity in ligand functionalization. Increased precision, however, presents major challenges for synthesis.[10,68] This is because surface patterning relies on grafts segregation and thus are restricted by the intrinsic NP core geometry. Along this vein, polymer scaling

Figure 6. Stimuli-driven patchy nanoparticle (PNP) formation. Changing solvent quality can cause drastic changes in chain conformation of grafted polymer brushes on NP surfaces. (a) Chain collapse drives formation of local patches on NP surfaces.[80] (b) Interplay between closely confined patches can drive chiral patch patterning.[81] (c) Metallic NP can be polarized under an external field to induce directional interaction that varies with field strength. Strong field induces strong dipole–dipole interactions, producing emergent patchiness and directionality in ellipsoid assembly.[75]

theories exist that provide strategies to bypass constraints due to NP shape. Scaling theories have been developed to predict poor solvent-induced patch formation[80] as well as chain–chain-mediated patch localization[10] as a function of experimentally relevant parameters. Another avenue looks at using block polymer ligand architectures to take advantage of microphase separation to produce spontaneous pattern formation NP surfaces.[82] Furthermore, rigorous theories have been developed to describe the emergent valency in ligand-functionalized NPs due to local crowding between neighbors,[83] giving rise to valency and patchiness on otherwise isotropic LNPs. These theoretical tools can provide a blueprint to guide experimental design and synthesis of polymeric PNPs.

For protein-based NPs, computational tools exist for designing protein interactions that focus on protein–protein, protein–ligand, and short oligomeric grafts.[71,84–87] However, there are still open challenges. Polymers/DNA grafts are similar in size or larger than the protein cores, pushing these systems beyond the scope of current design capabilities.[46,88] Some preliminary works have looked at polymer adsorption to protein surfaces, but these studies focus on polymer interactions with a single protein and not self-assembly.[89] To properly understand polymer/DNA chain interactions with protein cores and predict the emergent patchiness of the grafted proteins, several assumptions must be relaxed: (1) The core is assumed to be convex, (2) all surface sites are assumed to be chemically identical, and (3) the core is assumed to be rigid. Currently, no theoretical guidance exists to provide insight into how such features can influence site selectivity for ligand functionalization. Development of theories describing these effects will provide a fundamental understanding of the complex interplay between protein shape, surface charge, chain architecture, and graft location in controlling the emergent patchiness of polymer/DNA-functionalized proteins for use in directed self-assembly.

Conclusion

Major advances in synthesis over the last decade have enabled the fabrication of more complex surface patterning to create a synthetic suite of PNPs. These PNPs span a diverse range of material types that include polymeric amphiphiles, metallic nanocrystals, DNA/RNA origami, proteins, and ligand-functionalized nanocrystals/proteins. Successful integration between theory, simulation, and experiments will map out effective strategies for creating versatile PNPs from among the classes of materials covered in this article. Doing so will expand the suite of accessible nanoscale superlattices and help lay the foundation for multifunctional nanoscale materials with applications across a wide range of industries. Examples include the following: (1) constructing ordered enzyme lattices where DNA tunes the domain spacing to develop highly selective biocatalytic membranes, or (2) employing polymer/DNA to create nanoparticle complexes that merge light harvesting and chiral properties together for applications in light detection and ranging devices, or (3) merging flexibility intrinsic to polymers with thermoelectric nanoparticles to create materials with high power density and energy generation capabilities for wearable electronics. In short, PNPs provide an ideal class of nanoscale synthons capable of achieving even the most complex of designer materials. Future advances in PNP design and synthesis will expand the suite of accessible nanoscale superlattices, opening

new avenues for the application of nanotechnology and nanofabrication techniques toward the grand materials challenges of our generation.

Acknowledgments

Author contributions
T.V. led the manuscript development and wrote the manuscript.

Funding

Data availability
Not applicable.

Code availability
Not applicable.

Conflict of interest
There is no conflict of interest.

Ethical approval
Not applicable.

References
1. M.A. Boles, M. Engel, D.V. Talapin, *Chem. Rev.* **116**, 11220 (2016). https://doi.org/10.1021/ACS.CHEMREV.6B00196
2. C.A. Mirkin, S.H. Petrosko, *ACS Nano* **17**(17), 16291 (2023). https://doi.org/10.1021/ACSNANO.3C06564
3. J.S. Kahn, O. Gang, *Angew. Chem. Int. Ed.* **61**(3), e202105678 (2022). https://doi.org/10.1002/ANIE.202105678
4. L. Sun, H. Lin, K.L. Kohlstedt, G.C. Schatz, C.A. Mirkin, *Proc. Natl. Acad. Sci. U.S.A.* **115**, 7242 (2018). https://doi.org/10.1073/PNAS.1800106115
5. F. Liu, Y. Li, Y. Huang, A. Tsyrenova, K. Miller, L. Zhou, H. Qin, S. Jiang, *Nano Lett.* **20**(12), 8773 (2020). https://doi.org/10.1021/ACS.NANOLETT.0C03641
6. X. Ma, K. Hahn, S. Sanchez, *J. Am. Chem. Soc.* **137**(15), 4976 (2015). https://doi.org/10.1021/JACS.5B02700
7. K.C. Elbert, T. Vo, D. Oh, H. Bharti, S.C. Glotzer, C.B. Murray, *ACS Nano* **16**, 4508 (2022). https://doi.org/10.1021/ACSNANO.1C10922
8. D. Zhao, V. Gimenez-Pinto, A.M. Jimenez, L. Zhao, J. Jestin, S.K. Kumar, B. Kuei, E.D. Gomez, A.S. Prasad, L.S. Schadler, M.M. Khani, B.C. Benicewicz, *ACS Cent. Sci.* **3**, 751 (2017). https://doi.org/10.1021/ACSCENTSCI.7B00157
9. Y.J. Kim, J.H. Kim, I.S. Jo, D.J. Pine, S. Sacanna, G.R. Yi, *J. Am. Chem. Soc.* **143**, 13175 (2021). https://doi.org/10.1021/JACS.1C05123
10. A. Kim, T. Vo, H. An, P. Banerjee, L. Yao, S. Zhou, C. Kim, D.J. Milliron, S.C. Glotzer, Q. Chen, *Nat. Commun.* **13**, 6774 (2022). https://doi.org/10.1038/s41467-022-34246-0
11. F.S. Bates, G.H. Fredrickson, *Annu. Rev. Phys. Chem.* **41**, 525 (2003). https://doi.org/10.1146/ANNUREV.PC.41.100190.002521
12. A.L. Ferguson, Y. Ma, J.C. Aulicino, *J. Phys. Chem. B* **125**, 2398 (2021). https://doi.org/10.1021/ACS.JPCB.0C08723
13. S. Lee, T. Vo, S.C. Glotzer, *Nat. Chem.* **15**, 905 (2023). https://doi.org/10.1038/s41557-023-01200-6
14. V. Bernales, M.A. Ortuño, D.G. Truhlar, C.J. Cramer, L. Gagliardi, *ACS Cent. Sci.* **4**, 5 (2018). https://doi.org/10.1021/ACSCENTSCI.7B00500
15. M. Huang, C.H. Hsu, J. Wang, S. Mei, X. Dong, Y. Li, M. Li, H. Liu, W. Zhang, T. Aida, W.B. Zhang, K. Yue, S.Z.D. Cheng, *Science* **348**, 424 (2015). https://doi.org/10.1126/SCIENCE.AAA2421
16. Z. Su, C.H. Hsu, Z. Gong, X. Feng, J. Huang, R. Zhang, Y. Wang, J. Mao, C. Wesdemiotis, T. Li, S. Seifert, W. Zhang, T. Aida, M. Huang, S.Z.D. Cheng, *Nat. Chem.* **11**, 899 (2019). https://doi.org/10.1038/s41557-019-0330-x
17. K. Yue, M. Huang, R.L. Marson, J. Hec, J. Huang, Z. Zhou, J. Wang, C. Liu, X. Yan, K. Wu, Z. Guo, H. Liu, W. Zhang, P. Ni, C. Wesdemiotis, W.B. Zhang, S.C. Glotzer, S.Z.D. Cheng, *Proc. Natl. Acad. Sci. U.S.A.* **113**, 14195 (2016). https://doi.org/10.1073/PNAS.1609422113
18. Y. Liu, T. Liu, Yan, X. Yun, Q.Y. Guo, J. Wang, R. Zhang, S. Zhang, Z. Su, J. Huang, G.X. Liu, W. Zhang, T. Aida, K. Yue, M. Huang, S.Z.D. Cheng, *Giant* (Oxford) **4**, 100031 (2020). https://doi.org/10.1016/J.GIANT.2020.100031
19. Z. Su, R. Zhang, X.Y. Yan, Q.Y. Guo, J. Huang, W. Shan, Y. Liu, T. Liu, M. Huang, S.Z.D. Cheng, *Prog. Polym. Sci.* **103**, 101230 (2020). https://doi.org/10.1016/J.PROGPOLYMSCI.2020.101230
20. J. Zhu, M. Li, R. Rogers, W. Meyer, R.H. Ottewill, W.B. Russel, P.M. Chaikin, *Nature* **387**, 883 (1997). https://doi.org/10.1038/43141
21. A.J. Mueller, A.P. Lindsay, A. Jayaraman, S. Weigand, T.P. Lodge, M.K. Mahanthappa, F.S. Bates, *Macromolecules* **55**(18), 8332 (2022). https://doi.org/10.1021/ACS.MACROMOL.2C01267
22. S.A. Kim, K.J. Jeong, A. Yethiraj, M.K. Mahanthappa, *Proc. Natl. Acad. Sci. U.S.A.* **114**, 4072 (2017). https://doi.org/10.1073/PNAS.1701608114
23. A. Vidyasagar, S.H. Ku, M. Kim, M. Kim, H.S. Lee, T.R. Pearce, A.V. McCormick, F.S. Bates, E. Kokkoli, *ACS Macro Lett.* **6**, 1134 (2017). https://doi.org/10.1021/ACSMACROLETT.7B00523
24. A.K. Pearce, T.R. Wilks, M.C. Arno, R.K. O'Reilly, *Nat. Rev. Chem.* **5**, 21 (2020). https://doi.org/10.1038/s41570-020-00232-7
25. U. Agarwal, F.A. Escobedo, *Nat. Mater.* **10**, 230 (2011). https://doi.org/10.1038/nmat2959
26. T. Vo, S.C. Glotzer, *Proc. Natl. Acad. Sci. U.S.A.* **119**, e2116414119 (2022). https://doi.org/10.1073/PNAS.2116414119
27. G. Van Anders, N.K. Ahmed, R. Smith, M. Engel, S.C. Glotzer, *ACS Nano* **8**, 931 (2014). https://doi.org/10.1021/NN4057353
28. D. Caruntu, T. Rostamzadeh, T. Costanzo, S. Salemizadeh Parizi, G. Caruntu, *Nanoscale* **7**, 12955 (2015). https://doi.org/10.1039/C5NR00737B
29. J. Henzie, M. Grünwald, A. Widmer-Cooper, P.L. Geissler, P. Yang, *Nat. Mater.* **11**, 131 (2011). https://doi.org/10.1038/nmat3178
30. B.T. Diroll, X. Ma, Y. Wu, C.B. Murray, *Nano Lett.* **17**, 6501 (2017). https://doi.org/10.1021/ACS.NANOLETT.7B03123
31. S. Zhou, J. Li, J. Lu, H. Liu, J.Y. Kim, A. Kim, L. Yao, C. Liu, C. Qian, Z.D. Hood, X. Lin, W. Chen, T.E. Gage, I. Arslan, A. Travesset, K. Sun, N.A. Kotov, Q. Chen, *Nature* **612**, 259 (2022). https://doi.org/10.1038/s41586-022-05384-8
32. Y. Wang, J. Chen, R. Li, A. Götz, D. Drobek, T. Przybilla, S. Hübner, P. Pelz, L. Yang, B. Apeleo Zubiri, E. Spiecker, M. Engel, X. Ye, *J. Am. Chem. Soc.* **145**, 17902 (2023). https://doi.org/10.1021/JACS.3C05299
33. X. Ye, J.A. Millan, M. Engel, J. Chen, B.T. Diroll, S.C. Glotzer, C.B. Murray, *Nano Lett.* **13**, 4980 (2013). https://doi.org/10.1021/NL403149U
34. J. Kim, X. Song, F. Ji, B. Luo, N.F. Ice, Q. Liu, Q. Zhang, Q. Chen, *Nano Lett.* **17**, 3270 (2017). https://doi.org/10.1021/ACS.NANOLETT.7B00958
35. D. Frenkel, *Nat. Mater.* **14**, 9 (2014). https://doi.org/10.1038/nmat4178
36. J.M. Hodges, J.R. Morse, M.E. Williams, R.E. Schaak, *J. Am. Chem. Soc.* **137**, 15493 (2015). https://doi.org/10.1021/JACS.5B10254
37. S. Yang, R.A. LaCour, Y.Y. Cai, J. Xu, D.J. Rosen, Y. Zhang, C.R. Kagan, S.C. Glotzer, C.B. Murray, *J. Am. Chem. Soc.* **145**, 6280 (2023). https://doi.org/10.1021/JACS.2C12993
38. H. Zhu, Z. Fan, Y. Yuan, M.A. Wilson, K. Hills-Kimball, Z. Wei, J. He, R. Li, M. Grünwald, O. Chen, *Nano Lett.* **18**, 5049 (2018). https://doi.org/10.1021/ACS.NANOLETT.8B01860
39. H. Zhu, Z. Fan, S. Song, D. Eggert, Y. Liu, W. Shi, Y. Yuan, K.S. Kim, M. Grünwald, O. Chen, *ACS Nano* **16**, 15053 (2022). https://doi.org/10.1021/ACSNANO.2C06167
40. A.D. Terna, E.E. Elemike, J.I. Mbonu, O.E. Osafile, R.O. Ezeani, *Mater. Sci. Eng. B* **272**, 115363 (2021). https://doi.org/10.1016/J.MSEB.2021.115363
41. N.A. Lynd, A.J. Meuler, M.A. Hillmyer, *Prog. Polym. Sci.* **33**, 875 (2008). https://doi.org/10.1016/J.PROGPOLYMSCI.2008.07.003
42. B. Luo, A. Kim, J.W. Smith, Z. Ou, Z. Wu, J. Kim, Q. Chen, *Nat. Commun.* **10**, 1815 (2019). https://doi.org/10.1038/s41467-019-09787-6
43. M.S. Lawrence, K.J. Phillips, D.R. Liu, *J. Am. Chem. Soc.* **129**, 10110 (2007). https://doi.org/10.1021/JA071641Y
44. S. Zhang, R.G. Alberstein, J.J. De Yoreo, F.A. Tezcan, *Nat. Commun.* **11**, 3770 (2020). https://doi.org/10.1038/s41467-020-17562-1
45. D. Wu, N. Sinha, J. Lee, B.P. Sutherland, N.I. Halaszynski, Y. Tian, J. Caplan, H.V. Zhang, J.G. Saven, C.J. Kloxin, D.J. Pochan, *Nature* **574**, 658 (2019). https://doi.org/10.1038/s41586-019-1683-4
46. Y. Suzuki, G. Cardone, D. Restrepo, P.D. Zavattieri, T.S. Baker, F.A. Tezcan, *Nature* **533**, 369 (2016). https://doi.org/10.1038/nature17633
47. S. Gonen, F. DiMaio, T. Gonen, D. Baker, *Science* **348**, 1365 (2015). https://doi.org/10.1126/SCIENCE.AAA9897
48. C.M. Rufo, Y.S. Moroz, O.V. Moroz, J. Stöhr, T.A. Smith, X. Hu, W.F. Degrado, I.V. Korendovych, *Nat. Chem.* **6**, 303 (2014). https://doi.org/10.1038/nchem.1894
49. R.V. Rughani, D.A. Salick, M.S. Lamm, T. Yucel, D.J. Pochan, J.P. Schneider, *Biomacromolecules* **10**(5), 1295 (2009). https://doi.org/10.1021/BM900113Z
50. J.D. Brodin, X.I. Ambroggio, C. Tang, K.N. Parent, T.S. Baker, F.A. Tezcan, *Nat. Chem.* **4**, 375 (2012). https://doi.org/10.1038/nchem.1290
51. Z. Chen, M.C. Johnson, J. Chen, M.J. Bick, S.E. Boyken, B. Lin, J.J. De Yoreo, J.M. Kollman, D. Baker, F. Dimaio, *J. Am. Chem. Soc.* **141**, 8891 (2019). https://doi.org/10.1021/JACS.9B01978

52. Y.T. Lai, E. Reading, G.L. Hura, K.L. Tsai, A. Laganowsky, F.J. Asturias, J.A. Tainer, C.V. Robinson, T.O. Yeates, *Nat. Chem.* **6**, 1065 (2014). https://doi.org/10.1038/nchem.2107

53. Y. Hsia, J.B. Bale, S. Gonen, D. Shi, W. Sheffler, K.K. Fong, U. Nattermann, C. Xu, P.S. Huang, R. Ravichandran, S. Yi, T.N. Davis, T. Gonen, N.P. King, D. Baker, *Nature* **535**, 136 (2016). https://doi.org/10.1038/nature18010

54. P.W.K. Rothemund, *Nature* **440**, 297 (2006). https://doi.org/10.1038/nature04586

55. M.F. Parsons, M.F. Allan, S. Li, T.R. Shepherd, S. Ratanalert, K. Zhang, K.M. Pullen, W. Chiu, S. Rouskin, M. Bathe, *Nat. Commun.* **14**, 382 (2023). https://doi.org/10.1038/s41467-023-36156-1

56. C. Geary, G. Grossi, E.K.S. McRae, P.W.K. Rothemund, E.S. Andersen, *Nat. Chem.* **13**, 549 (2021). https://doi.org/10.1038/s41557-021-00679-1

57. X. Wang, S. Li, H. Jun, T. John, K. Zhang, H. Fowler, J.P.K. Doye, W. Chiu, M. Bathe, *Sci. Adv.* **8**, 39 (2022). https://doi.org/10.1126/SCIADV.ABN0039

58. M. Wang, L. Dai, J. Duan, Z. Ding, P. Wang, Z. Li, H. Xing, Y. Tian, *Angew. Chem.* **132**, 6451 (2020). https://doi.org/10.1002/ANGE.201913958

59. Y. Wang, L. Dai, Z. Ding, M. Ji, J. Liu, H. Xing, X. Liu, Y. Ke, C. Fan, P. Wang, Y. Tian, *Nat. Commun.* **12**, 3011 (2021). https://doi.org/10.1038/s41467-021-23332-4

60. Y. Tian, J.R. Lhermitte, L. Bai, T. Vo, H.L. Xin, H. Li, R. Li, M. Fukuto, K.G. Yager, J.S. Kahn, Y. Xiong, B. Minevich, S.K. Kumar, O. Gang, *Nat. Mater.* **19**, 789 (2020). https://doi.org/10.1038/s41563-019-0550-x

61. Y. Tian, Y. Zhang, T. Wang, H.L. Xin, H. Li, O. Gang, *Nat. Mater.* **15**, 654 (2016). https://doi.org/10.1038/nmat4571

62. W. Liu, M. Tagawa, H.L. Xin, T. Wang, H. Emamy, H. Li, K.G. Yager, F.W. Starr, A.V. Tkachenko, O. Gang, *Science* **351**, 582 (2016). https://doi.org/10.1126/SCIENCE.AAD2080

63. E.V. Shevchenko, D.V. Talapin, N.A. Kotov, S. O'Brien, C.B. Murray, *Nature* **439**, 55 (2006). https://doi.org/10.1038/nature04414

64. S.K. Kumar, B.C. Benicewicz, R.A. Vaia, K.I. Winey, *Macromolecules* **50**, 714 (2017). https://doi.org/10.1021/ACS.MACROMOL.6B02330

65. D. Samanta, W. Zhou, S.B. Ebrahimi, S.H. Petrosko, C.A. Mirkin, *Adv. Mater.* **34**, 2107875 (2022). https://doi.org/10.1002/ADMA.202107875

66. F. Lu, T. Vo, Y. Zhang, A. Frenkel, K.G. Yager, S. Kumar, O. Gang, *Sci. Adv.* **5**, 2399 (2019). https://doi.org/10.1126/SCIADV.AAW2399

67. K.C. Elbert, T. Vo, N.M. Krook, W. Zygmunt, J. Park, K.G. Yager, R.J. Composto, S.C. Glotzer, C.B. Murray, *ACS Nano* **13**, 14241 (2019). https://doi.org/10.1021/ACSNANO.9B07348

68. G. Chen, K.J. Gibson, D. Liu, H.C. Rees, J.H. Lee, W. Xia, R. Lin, H.L. Xin, O. Gang, Y. Weizmann, *Nat. Mater.* **18**, 169 (2018). https://doi.org/10.1038/s41563-018-0231-1

69. Y. Xiong, S. Yang, Y. Tian, A. Michelson, S. Xiang, H. Xin, O. Gang, *ACS Nano* **14**, 6823 (2020). https://doi.org/10.1021/ACSNANO.0C00607

70. J.R. McMillan, O.G. Hayes, P.H. Winegar, C.A. Mirkin, *J. Am. Chem. Soc.* **143**, 8925 (2021). https://doi.org/10.1021/JACS.1C04191

71. B.E. Partridge, P.H. Winegar, Z. Han, C.A. Mirkin, *J. Am. Chem. Soc.* **143**, 8925 (2021). https://doi.org/10.1021/JACS.1C04191

72. O.G. Hayes, B.E. Partridge, C.A. Mirkin, *Proc. Natl. Acad. Sci. U.S.A.* **118**, e2106808118 (2021). https://doi.org/10.1073/PNAS.2106808118

73. O.G. Hayes, J.R. McMillan, B. Lee, C.A. Mirkin, *J. Am. Chem. Soc.* **140**, 9269 (2018). https://doi.org/10.1021/JACS.8B05640

74. J. Zhou, M.N. Creyer, A. Chen, W. Yim, R.P.M. Lafleur, T. He, Z. Lin, M. Xu, P. Abbasi, J. Wu, T.A. Pascal, F. Caruso, J.V. Jokerst, *J. Am. Chem. Soc.* **143**, 12138 (2021). https://doi.org/10.1021/JACS.1C04272

75. R.S. Hendley, I. Torres-Díaz, M.A. Bevan, *Soft Matter* **17**, 9066 (2021). https://doi.org/10.1039/D1SM01227D

76. J.J. Juárez, S.E. Feicht, M.A. Bevan, *Soft Matter* **8**, 94 (2011). https://doi.org/10.1039/C1SM06414B

77. R.S. Hendley, L. Zhang, M.A. Bevan, *Soft Matter* **18**, 9273 (2022). https://doi.org/10.1039/D2SM01078J

78. I. Torres-Díaz, B. Rupp, Y. Yang, M.A. Bevan, *Soft Matter* **14**, 934 (2018). https://doi.org/10.1039/C7SM02287E

79. E. Galati, M. Tebbe, A. Querejeta-Fernández, H.L. Xin, O. Gang, E.B. Zhulina, E. Kumacheva, *ACS Nano* **11**, 4995 (2017). https://doi.org/10.1021/ACSNANO.7B01669

80. R.M. Choueiri, E. Galati, H. Thérien-Aubin, A. Klinkova, E.M. Larin, A. Querejeta-Fernández, L. Han, H.L. Xin, O. Gang, E.B. Zhulina, M. Rubinstein, E. Kumacheva, *Nature* **538**, 79 (2016). https://doi.org/10.1038/nature19089

81. E. Galati, H. Tao, M. Tebbe, R. Ansari, M. Rubinstein, E.B. Zhulina, E. Kumacheva, *Angew. Chem. Int. Ed.* **58**, 3123 (2019). https://doi.org/10.1002/ANIE.201812887

82. T. Vo, *AIChE J.* **69**(12), e18243 (2023). https://doi.org/10.1002/AIC.18243

83. J. Hallstrom, I. Cherniukh, X. Zha, M.V. Kovalenko, A. Travesset, *ACS Nano* **17**, 7219 (2023). https://doi.org/10.1021/ACSNANO.2C10079

84. S.L. Kuan, F.R.G. Bergamini, T. Weil, *Chem. Soc. Rev.* **47**, 9069 (2018). https://doi.org/10.1039/C8CS00590G

85. Y. Shen, A. Levin, A. Kamada, Z. Toprakcioglu, M. Rodriguez-Garcia, Y. Xu, T.P.J. Knowles, *ACS Nano* **15**, 5819 (2021). https://doi.org/10.1021/ACSNANO.0C08510

86. N. Stephanopoulos, *Chem* **6**, 364 (2020). https://doi.org/10.1016/J.CHEMPR.2020.01.012

87. S. Zhang, *Nat. Biotechnol.* **21**, 1171 (2003). https://doi.org/10.1038/nbt874

88. W.J. Song, F.A. Tezcan, *Science* **346**, 1525 (2014). https://doi.org/10.1126/SCIENCE.1259680

89. B. Panganiban, B. Qiao, T. Jiang, C. DelRe, M.M. Obadia, T.D. Nguyen, A.A.A. Smith, A. Hall, I. Sit, M.G. Crosby, P.B. Dennis, E. Drockenmuller, M.O. De La Cruz, T. Xu, *Science* **359**, 1239 (2018). https://doi.org/10.1126/SCIENCE.AAO0335

90. H. Zhu, Z. Fan, L. Yu, M.A. Wilson, Y. Nagaoka, D. Eggert, C. Cao, Y. Liu, Z. Wei, X. Wang, J. He, J. Zhao, R. Li, Z. Wang, M. Grünwald, O. Chen, *J. Am. Chem. Soc.* **141**, 6013 (2019). https://doi.org/10.1021/JACS.9B01033

91. R. Veneziano, S. Ratanalert, K. Zhang, F. Zhang, H. Yan, W. Chiu, M. Bathe, *Science* **352**(6293), 1534 (2016). https://doi.org/10.1126/SCIENCE.AAF4388

92. J.D. Brodin, E. Auyeung, C.A. Mirkin, *Proc. Natl. Acad. Sci. U.S.A.* **112**, 4564 (2015). https://doi.org/10.1073/PNAS.1503533112

Publisher's note

Thi Vo is an assistant professor of chemical and biomolecular engineering at Johns Hopkins University. He received his BS degree from Rice University and PhD degree from Columbia University. He was a postdoctoral researcher at the University of Michigan and has been at Johns Hopkins University since 2022. He is a theoretician who specializes in polymer and nanoscale self-assembly. His group develops insights into fundamental interactions to guide the design of complex building blocks for materials fabrication. Vo can be reached by email at tvo12@jhu.edu.